Engineered Science
DOI: https://dx.doi.org/10.30919/es1008

Establishing Efficacy of Machine Learning Techniques for Vulnerability Information of Tubular Buildings

Muhammad Zain,[1] Suraparb Keawsawasvong,[2] Chanachai Thongchom,[2] Issara Sereewatthanawut,[3,*] Muhammad Usman[4] and Lapyote Prasittisopin[1,*]

Abstract

During recent times, the emergence of artificial intelligence in structural engineering has rendered researchers to work on reducing the overall computational effort required for producing vulnerability information of infrastructural facilities. However, the supertall and tubular building analysis lacks substantial research due to their intricate structural behavior and aleatory uncertainties. This paper establishes the feasibility of using versatile Machine Learning (ML) algorithms for producing fragility relationships of high-rise tubular structures by considering a 55-story tall building, located in high seismicity area. Initially, the vibrational modes are decoupled, and Incremental Dynamic Analysis (IDA) has been conducted on each individual mode discreetly. The initial four modes were considered for analysis, constituting overall modal mass participation of more than 90%. Inference has been drawn between the efficacy of employed ML techniques to establish grounds for rapid structural vulnerability assessment of high-rise buildings considering ground motion features along with the structural characteristics. Testing datasets have suggested the overall adequacy of ML algorithms by substantiating the successful prediction of Engineering Demand Parameter (EDP), and their applicability for establishing vulnerability information of high-rise structures.

Keywords: Machine learning; Vulnerability; Tabular building; BIM.
Received: 11 October 2023; Revised: 02 November 2023; Accepted: 03 November 2023.
Article type: Research article.

1. Introduction

The assessment of structural vulnerability of high-rise buildings has always been a computationally extensive task that faces substantial research gaps to address.[1,2] The information obtained from a vulnerability assessment process assists the pertinent emergency management departments to respond effectively in post-disaster situations.[3–5] Conventionally, the vulnerability information is portrayed in terms of fragility curves[6] Essentially, fragility curves depict the graphical information of the probability of being in a specific damage condition against discreet levels of seismic activity. There can be four types of fragility relationships *i.e.*, empirical, judgmental, analytical, and hybrid.[6–8] Empirical curves are dependent upon the experimental evidence of structural damage, and tangible examples of empirical fragility curves can be seen in the works.[9–11] Judgmental fragility curves are characterized by the technical judgement of experts predicting the structural vulnerability based upon their professional and research experiences. Such curves are established when the actually observed damage data is not available.[12–14] On the other hand, analytical fragility relationships require elaborate engineering analysis, and thus are computationally extensive, requiring significant computational resources, technical expertise, and time.[15] While several recent studies have attempted to establish the analytical fragility curves of structures withered by

[1]*Architectural Technology Research Unit, Department of Architecture, Faculty of Architecture, Chulalongkorn University, Bangkok, 10330, Thailand.*
[2] *Department of Civil Engineering, Thammasat School of Engineering, Faculty of Engineering, Thammasat University, Pathumthani, 12120, Thailand.*
[3] *King Prajadhipok's Institute, Bangkok 10210, Thailand.*
[4] *School of Civil and Environmental Engineering, National University of Sciences and Technology (NUST), Islamabad, 44000, Pakistan.*
**Email:* lapyote.p@chula.ac.th (L. Prasittisopin);
issara.se@kpi.ac.th (I. Sereewatthanawut)

simplifying the structural modelling[16,17] or by using simplified analysis techniques.[18,19] Similarly, hybrid fragility curves are those which are developed by combining either two or more categories of fragility curves. Conventionally, the analytical fragility curves are considered to be the most accurate ones as they involve elaborate nonlinear analysis; however, nonlinear dynamic analyses are computationally extensive and thus pose higher processing demands.[20]

More recently, the use of Artificial Intelligence (AI) has been increased in structural engineering applications primarily to address the extensive computational toll exerted by the analytical fragility assessment process.[21] The implementation of Machine Learning (ML) techniques enhances the data analyses capability and determines typical patterns for solving analogous problems.[22,23] Previous studies such as the ones conducted by Hameed *et al.*,[24] are tangible examples. The ML techniques are broadly categorized into two categories *i.e.*, Unsupervised Machine Learning (USML), and Supervised Machine Learning (SML). As their names suggest, USML does not need any supervision for training of the data model and is conventionally known as clustering; while SML algorithm utilizes labelled input and output data and is termed as classification because the data is classified in terms of inputs and outputs. SML algorithms iteratively make the data predictions by learning from the training sets with the help of labelled data *i.e.*, upfront human intervention, while USML algorithms require the human intervention to validate the output only after recognizing the intrinsic data patterns on their own.[25]

In structural engineering, both types of algorithms have been implemented. For instance, Mangalathu and Jeon[26] investigated the efficacy of various SML algorithms for predicting shear strength of joints in skeleton structures, and eventually concluded that Lasso Regressions resulted in better accuracy in comparison with other considered algorithms. Mangalathu and Jeon[27] established a framework for probabilistic seismic risk analysis using SML Artificial Neural Network (ANN) based on a ten-fold cross validation for building structures. Todorov and Billah[28] investigated the varying configurations of Canadian bridge piers and established numerous dataset models to evaluate the most suitable SML algorithm for post-earthquake seismic capacity estimation. On the other hand, the application of USML has been mostly implemented for structural optimization and damage detection. Wang and Cha[29] proposed unsupervised damage detection models for steel bridges and utilized four USML methods including Gaussian mixture model, density peaks clustering, one-class support vectors, and K-nearest neighbors. Similarly, Wen *et. al*.[30], Eltouny and Liang[31] and S. Shi *et. al*.[32] employed USML techniques including fuzzy logic, Bayesian-optimized learning, and K-nearest neighbor respectively for structural health monitoring and damage detection. The USML has also been used for structural models' optimization, and the works of Eltouny *et. al*.,[33] Mai *et. al*.,[34] Shin *et. al*.,[35] and Zhang *et. al*.[36] are apparent instances. However, most studies have only included either the seismic parameters or structural parameters to establish the structural responses though ML algorithms. Furthermore, no systematic study has specifically investigated the efficacy of SML and USML algorithms for assessing the vulnerability of high-rise tubular structures.

The current study aims to establish the efficacy of versatile ML techniques for predicting the seismic vulnerability of high-rise buildings, depending upon their structural features and varying seismic demands with distinct frequency distributions. Furthermore, the presented study focuses on comparing the performance of employed ML models with conventional engineering analysis so that their suitability and rational feasibility of implementation could be assessed to cope for extensive computational requirements and complexity of vulnerability assessment processes. Thus, the current study fundamentally differs from existing studies that target ML algorithms for vulnerability assessments as it does not consider conventional low-rise and mid-rise structures, rather it considers a 55-story high-rise tubular core-wall structure as a case study for establishing the efficacy of ML algorithms.

Unlike low-rise or medium-rise structures, tubular buildings have convoluted load distribution, stress concentrations, and dynamic responses with distinguished geometrical and structural characteristics. Due to their versatile range of motions, such buildings respond to both *i.e.*, low-frequency and high-frequency earthquakes due to the extensive involvement of their higher vibrational modes. Thus, tubular buildings require an intricate comprehension of nexus between distinctive structural behavior and stochastically independent seismic demands. Furthermore, numerous complexities including differentiating shear capping in different structural modes further complicate the analyzing of tubular buildings. Moreover, the supertall or tubular buildings exhibit higher geometrical nonlinearity, and composite materials' structure makes it further difficult to capture the actual behavior of the structural system. Such convoluted behavior of these structures, their nonlinearity, and the complex frame-wall interaction make it substantially difficult to conduct the seismic vulnerability assessment studies, and resultantly, the computational demands irrationally rise, and a single tubular building may take number of days to get

analyzed with reasonably accurate results.

Thus, despite simplifying the modelling and analysis techniques for high-rise structures, it is the need of the hour to establish such ML algorithms that can be implemented for a swift evaluation of structural vulnerability for such complex structures. Furthermore, a wholesome incorporation of seismic parameters along with the parametric structural configuration is imperative for establishing widely implementable ML algorithms that can incorporate the complexity between input parameters and buildings' overall performance. Thus, unlike most of the previous works, the presented work considers both *i.e.* the structural parameters as well as the seismic input parameters to train the models.

Initially, a full nonlinear 3-dimensional (3D) analytical model has been developed and subjected to nonlinear static and dynamic analysis to check its structural performance. Eventually, the vibrational modes are decoupled in accordance with the methodology presented in the work of Zain *et. al*.,[37] and Incremental Dynamic Analysis (IDA) has been performed on the decoupled modes to produce the results for ML algorithms training, validation and testing. Eventually, this paper explores the feasibility of employing ML techniques such as Artificial Neural Network (ANN), K-nearest Neighbor (KNN), Support Vector Machine (SVM), Decision Tree (DT), and Random Forest (RF) for seismic fragility assessment of high-rise tubular structures by incorporating both *i.e.*, the ground motions, as well as the structural features. The assessment of versatile ML algorithms has resulted in establishing their successful efficacy for predicting the structural vulnerability swiftly. The proceeding sections describe the establishing of 3D nonlinear model, the production of fragility curves based on engineering analysis, and development and training of ML algorithms for assessing structural vulnerability, considering the available results.

2. Structural modelling

A real-world 55-story tall building structure has been considered to establish the efficacy of ML algorithms for structural vulnerability assessment of tall buildings. The building was initially considered by Zain *et. al*.[37] for their research studies work. The nonlinear structural model has been developed in the CSI Perform 3D software package as the software provides excellent nonlinear modelling environment for complex core-wall structures and does not have any issues with the convergence of the solution. The building is situated in the seismically active region of Metro Manila, the largest metropolitan area of Philippines. It has the first four floors as the podium with floor area of 4991 m^2, while the typical floor area of tower floors is 1560 m^2. During structural modelling, the structural behavior of materials is considered to be following Hooke's Law; however, with the exceedance of yield strengths, the deviations from actual response could happen, which may potentially impact the accuracy of vulnerability predictions under severe seismic demands. Furthermore, the materials are assumed to follow the isotropic characteristics as deviations from isotropic properties may lead to differential structural deformations, which are not the point of focus for this study as the vulnerability assessment is made at global level. The geometrical features are mentioned in Table 1.

Table 1. Geometrical characteristics of building analyzed.

Feature	Description
Number of stories	55
Typical podium plan area	4991 m^2
Typical Floor plan area	1560 m^2
Total height	163 m

Figure 1 shows the typical framing plans for basement/ground and tower portion floors. The red color in Figs. 1(a) and 1(b) designates the shear walls in the considered building. The columns are designated through C-1 to C-12, while shear walls are designated through SW-1 to SW-4. The LB in Fig. 1(b) indicates the link beams. A typical elevation and x-sectional details specifically for link beams have been provided in Fig. 2. The construction materials strengths for different types of structural member are provided in Table 2 that depicts the values for employed concrete strength. For structural steel, Grade 60 reinforcing steel has been employed during analytical modelling process. For detailed structural x-sections variations of columns and shear walls along the height of the considered building, the readers of this work are referred to Zain *et. al*.[37]

Table 2. Material characteristics for structural components.

Structural Member		Concrete Strength (MPa)
Slabs, Beams & Girders	Base to 40th Floor Level	41
	40th to Roof Level	34
Shear Walls & Columns	Base to 11th Floor Level	69
	12th to 21st Floor Level	59
	21st to Roof Level	48

To model the nonlinearity, a fiber-based model of the structure was developed. The core wall was modeled completely nonlinear, and nonlinear fiber elements were

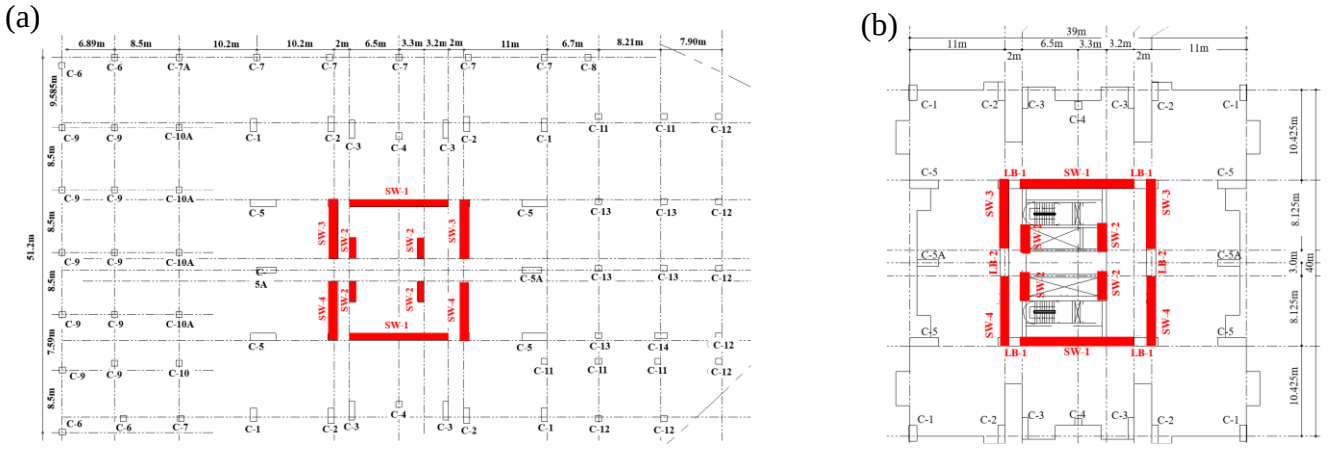

Fig. 1 Framing plans: (a) framing plan for basement and ground floors; (b) typical framing plan for tower floors.

employed to monitor the strains in the steel and concrete fibers of the shear wall to check the yielding and respective failure. The use of nonlinear fibers permitted to monitor the strains separately in the confined and unconfined regions and the composite behavior was integrated using the constitutive stress-strain relationship of materials. In the present work, Non-Buckling Inelastic Steel Material mode, available in CSI Perform 3D, was utilized to model the steel, while unconfined and confined concrete regions were modelled using Takeda and Mander Models respectively in CSI Perform 3D. The composite behavior of the structural members was ensured by implementing the constitutive stress-strain relationships of respective materials in nonlinear regions. The frame elements were also modeled nonlinear, however, instead of using the fiber elements, the nonlinear hinges were employed at respective ends of all nonlinear line elements to characterize their nonlinearity during nonlinear static and dynamic loading. For discreet details on nonlinearity considerations during modelling process, the readers are referred to the work of Zain *et. al*..[37] The established 3D nonlinear model is shown in Fig. 3.

2.1 Modal decomposition and nonlinear static analysis

The modal decomposition has been implemented in accordance with the procedure stated in Zain *et. al*.[37] and Chopra.[38] The primary objective of modal composition is to decrease the analysis runtime without losing the accuracy of results as analyzing full 3D nonlinear structure could be irrational because the runtime would have been excessively enormous. Since the primary objective of this paper is to establish the feasibility of employing ML algorithms for vulnerability assessment, therefore, the decomposition is not discussed here in detail, and the readers of this work are referred to Zain *et. al*.[37] to study the procedure of modal decomposition. In accordance with the procedure proposed in Chopra[38] and elaborated in Zain *et. al*.,[37] four vibrational modes were decomposed from the original structure, and were represented using Single Degree of Freedom (SDOF) systems with each system containing the force-deformation (F-D) relationship of its respective mode. The time period of each

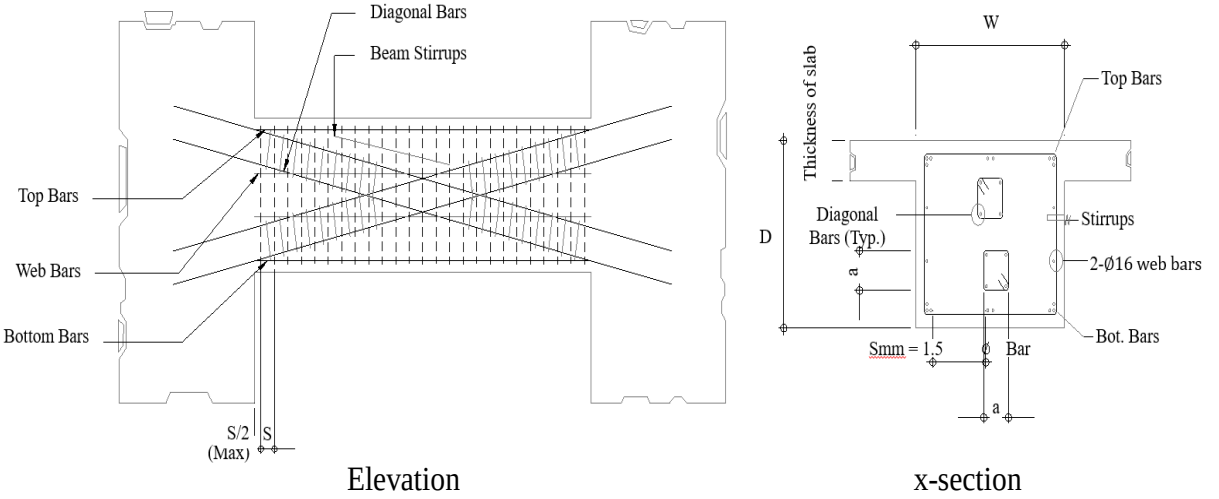

Fig. 2 Typical elevation and x-section of link beams.

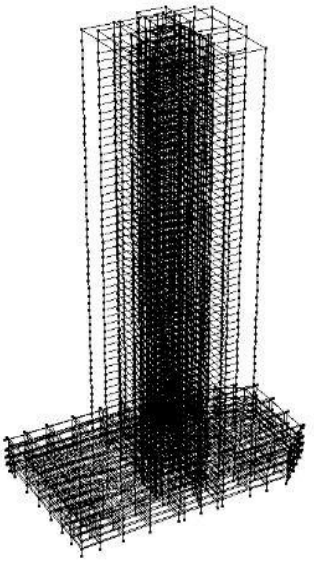

Fig. 3 3-Dimensional analytical model of the building in CSI Perform 3D.

considered mode was determined to be 4.76 sec., 1.12 sec., and 0.507 sec. respectively for first three modes. The number of modes taken into account were based upon considering that total modal mass participation ratio should be equal to or more than 90% as proposed by Chopra.[38] However, to establish the F-D relationships for SDOF systems, the monotonic and cyclic pushover analyses were conducted on the 3D nonlinear model in CSI Perform 3D by applying the forces in accordance with the modal shapes of the modes. For monotonic nonlinear static analysis, the applied force distributions are shown in Fig. 4 for the considered modes, while the obtained monotonic results are presented in Fig. 5.

The cyclic pushover curve for the considered structure is shown in the Fig. 6. Monotonic nonlinear static analysis had been required to establish the limit states of the structure for vulnerability assessment. The Limit States (LS), often known as Damage States, characterize the structural damage condition against the threshold values of an Engineering Demand Parameter (EDP). Different researchers have used different structural limit states with corresponding EDP to identify the pertaining structural condition. The details of the LS and EDP are discussed in the proceeding section.

2.2. Development and analysis of SDOF Structures

Global hysteretic relationship has been developed by subjecting the full 3D nonlinear model to cyclic loading so that the obtained cyclic behavior could be used in the SDOF systems for replicating the actual structural behavior, considering the strength and stiffness degradation characteristics. The global hysteretic relationship is shown in Fig. 6.

For establishing the SDOF systems, Interactive Interface for Incremental Dynamic Analysis Procedure (IIIDAP), developed by McGill University,[39] has been used. IIIDAP is a generic software package for analyzing SDOF systems. IIIDAP provides the convenience of implementing Incremental Dynamic Analysis (IDA) by permitting the increase in seismic intensities for each successive set of analysis. The software contains predefined sets of ground motions from which a user can select as per the requirements of analysis, and it also allows the user to use custom input ground motions after selecting from some other database. In the presented study, the SDOF systems have been developed using the IIIDAP interface. Since the IDA had been

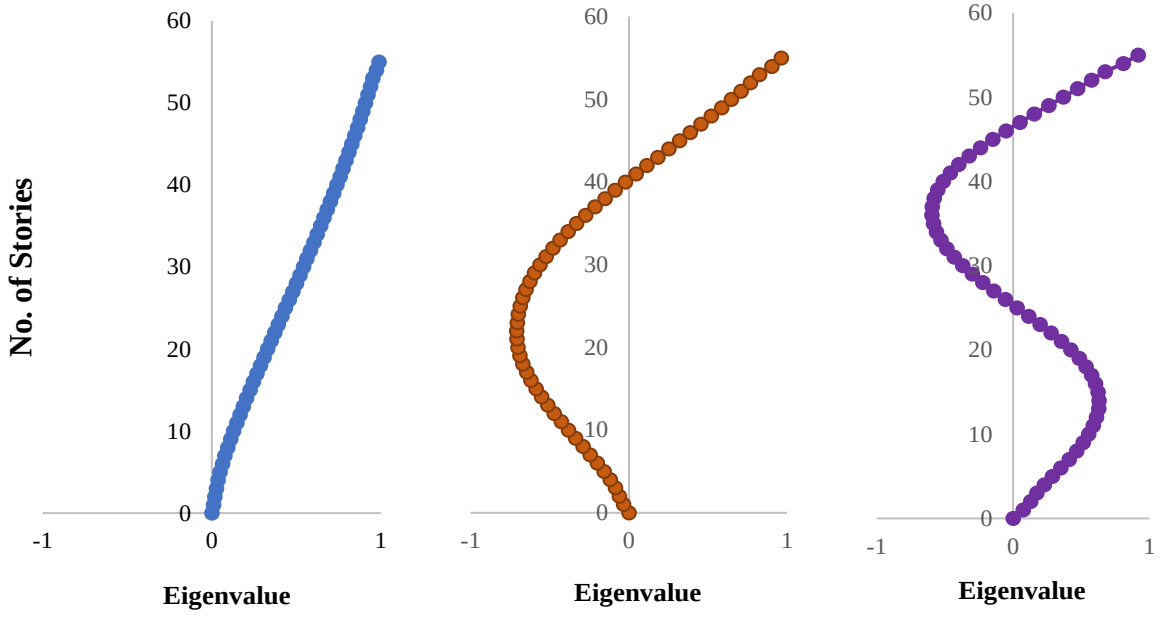

Fig. 4 Loading pattern for monotonic analysis in considered modes.

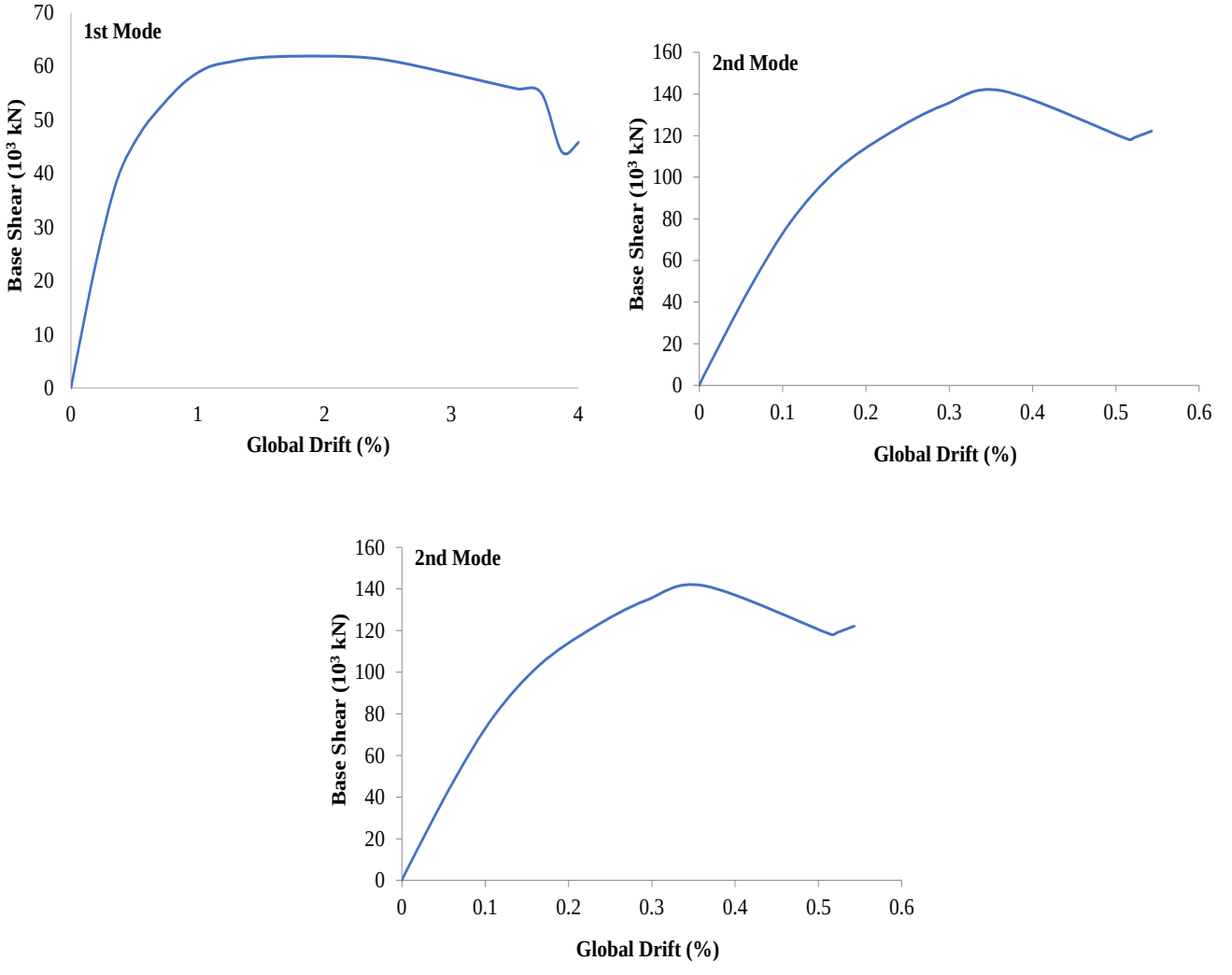

Fig. 5 Pushover curves for all three considered modes.

implemented on the SDOF systems to obtain a cumulative response as the representative of full structural response, it was imperative to compare the obtained results from SDOF systems with the response history obtained from 3D nonlinear model. Thus, the 3D nonlinear model and all the developed SDOF systems were subjected to a same ground motion history of Tabas, Iran, scaled to have the Peak Ground Acceleration (PGA) of 1.0 g. the Fig. 7 shows the comparison of result obtained from 3D nonlinear model and the collective result obtained from SDOF systems.

The comparison of responses in Fig. 7 reveals that the cumulative response obtained from the SDOF systems has been in good agreement with the response obtained from the 3D nonlinear structure with closely matching drift values. The differences in the curves are primarily attributed to the softness of the SDOF systems and the analyzing algorithm of IIIDAP that allows for the readjustment against stiffness degradation. However, despite the elongation of the time, the drift values have negligible differences, as indicated by the Fig. 7. Thus, the subsequent dynamic analyses have been performed using the established SDOF systems.

3. Incremental dynamic analysis (IDA)

Incremental Dynamic Analysis (IDA) is considered as one of the most sophisticated analysis techniques to establish vulnerability information of structures.[40] The fragility curves for the considered building have been developed using IDA of decoupled vibrational modes, constituting modal mass participation ratio of more than 90%. After the validation, IDA has been performed on each SDOF system separately, and after analyses the cumulative results have been evaluated by combining the responses obtained from each SDOF system in accordance with the following equation:

$$r(t) = \sum_{i=1}^{m} r_i\,(t) \quad (1)$$

In the above equation, the response of a SDOF systems is denoted by $r_i(t)$ for any n^{th} mode, while m represents the total number of modes considered. For better understanding of the desegregation of responses and their eventual amalgamation,

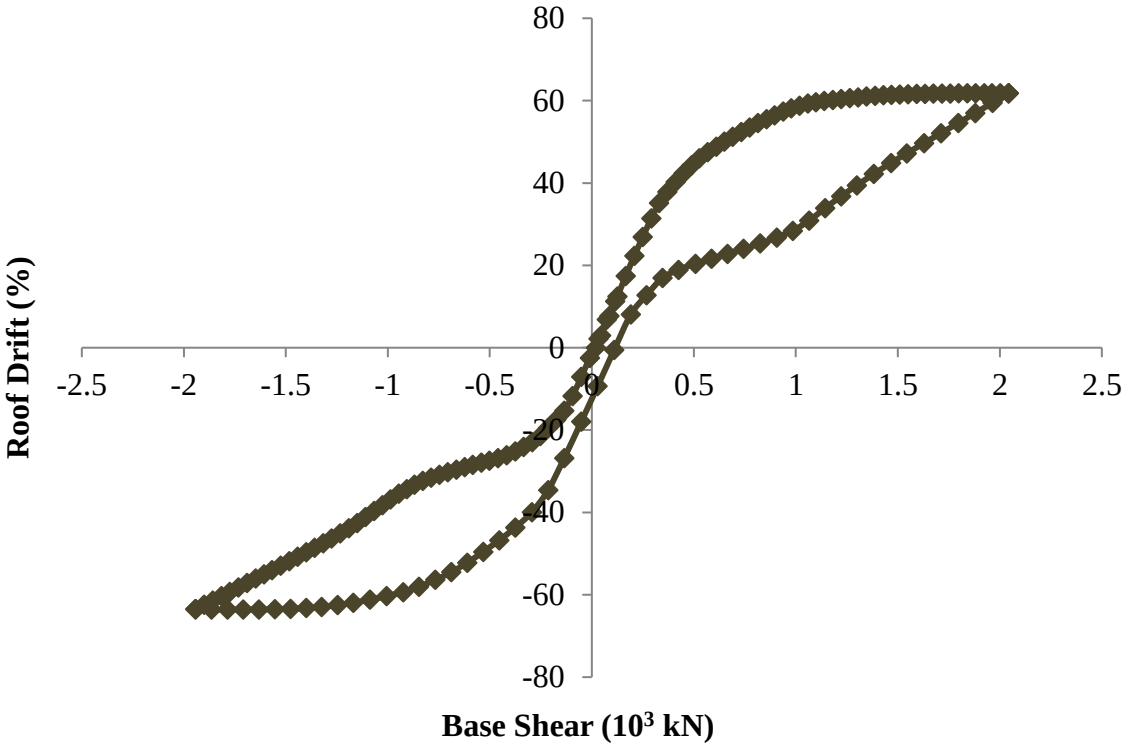

Fig. 6 Global Hysteretic Relationship.

the readers of this work are referred to study the works of M. Zain *et. al*.[37] For implementing IDA, it is imperative to define seismic intensity measures (IM) that can correlate the seismic intensity with structural damage. The proceeding section addresses the selection and the scaling of IMs in the current study.

3.1 Selection and scaling of ground motions and IM

IM correlate the structural damage with the seismic intensity. The most common IM used in the literature is the Peak Ground Acceleration (PGA) as it is easily comprehendible by the people with nontechnical background. However, D. D. Nguyen *et. al*.[41] and M. Grigoriu[42] has reported the Spectral Acceleration (Sa) as a better IM as PGA ignored the structural characteristics, while Sa took into account the structural features and thus, can correlate better with the structural damage. In the presented study, three IMs have been used *i.e.* PGA, Sa @ 1 sec., and Sa @ 0.2 sec. Spectral accelerations at different periods have been used because a tall building can experience seismic excitations in different structural modes in accordance with the frequency distribution of the ground motions and considering the Sa at 1.0 sec. and 0.2 sec. allows to over both low- and high-frequency responses. In the present work, the selected ground motions are incrementally scaled at discreet levels of 0.1 g up to 2.0 g. In this work, 15 large natural ground motions have been meticulously selected. The ground motions were selected from the robust PEER Ground Motions database, NGA-West2 that offers splendid control over the GM selection features including the source mechanism, shear wave velocities in the upper 30 m of earth's crest (V_{s30}), and distance to rupture to refine the selection process. The GM database possesses a substantially large record of different seismic motions in active seismic regions across the globe, with a particular focus on shallow crustal

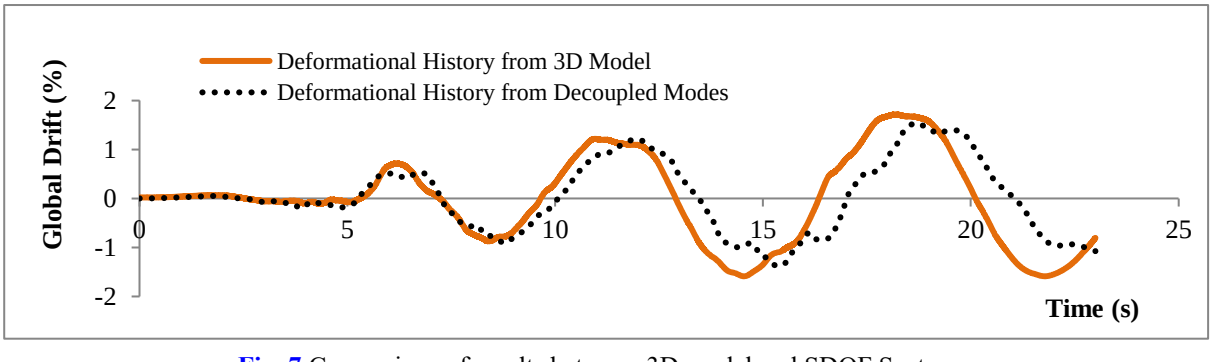

Fig. 7 Comparison of results between 3D model and SDOF Systems.

earthquakes. In the current study, larger ground motions have been selected having magnitudes larger than 5.0 to 8.0. However, near-to-source and distant-to-source, both sorts of earthquake are selected to cover far field and near field responses, while distance to rupture varies in between 1 to 90 km to capture the both *i.e.*, low-frequency and higher-frequency responses. The source mechanism has not been considered for the selection, rather all types of source mechanisms *i.e.*, strike slip, thrusts, reverse faults, etc. have been considered to capture the diversity of in seismic ground motions to ensure the generalization. Since the primary focus of the study is to establish the wholesome efficacy of ML algorithms for tubular structures, therefore the GM selection has been made considering both stiff and soft soil conditions to include varying path attenuation relationships to ensure the algorithms are developed with real-world representativeness of the data for structural vulnerability assessment. Table 3 presents the natural ground motions (GMs) selected in this work. Fig. 8 shows the developed spectra of selected GMs with 5% damping. The black bold line in the figure exhibits the average spectra of selected ground motions.

3.2 Hazard-Damage relationship

IDA results in producing hazard-damage relationships. Since three IMs have been considered in the presented study, there different results were shown. A total of 2700 analyses were conducted discreetly *i.e.*, 900 analyses run against each SDOF System (300 analyses for each IM on a single SDOF System). The peak drifts obtained from the analysis after obtaining the cumulative results are shown in Fig. 9, which substantiates

Table 3. Selected ground motions.

Sr. No.	Earthquake Location	Distance to rupture (km)	Magnitude (Mw)	PGA (g)
GM 1	Aftershock of Friuli EQ, Italy	10	5.7	0.2305
GM 2	Alkion, Greece	25	6.1	0.1199
GM 3	Anza (Horse Cany)	20.6	5.0	0.097
GM 4	Caolinga	12.6	5.0	0.673
GM 5	Chi-Chi, Taiwan	7.31	7.6	0.821
GM 6	Chi-Chi, Taiwan	39.34	7.6	0.088
GM 7	Dinar, Turkey	1.0	6.0	0.3193
GM 8	Imperial Valley	2.5	6.5	0.775
GM 9	Kobe, Japan	1.2	6.9	0.694
GM 10	Kobe, Japan	89.3	6.9	0.081
GM 11	Kocaeli, Turkey	76.1	7.4	0.179
GM 12	Kocaeli, Turkey	78.9	7.4	0.249
GM 13	Loma Prieta, USA	5.1	6.9	0.644
GM 14	Northridge	17.5	6.7	1.779
GM 15	Northridge	64.6	6.7	0.139

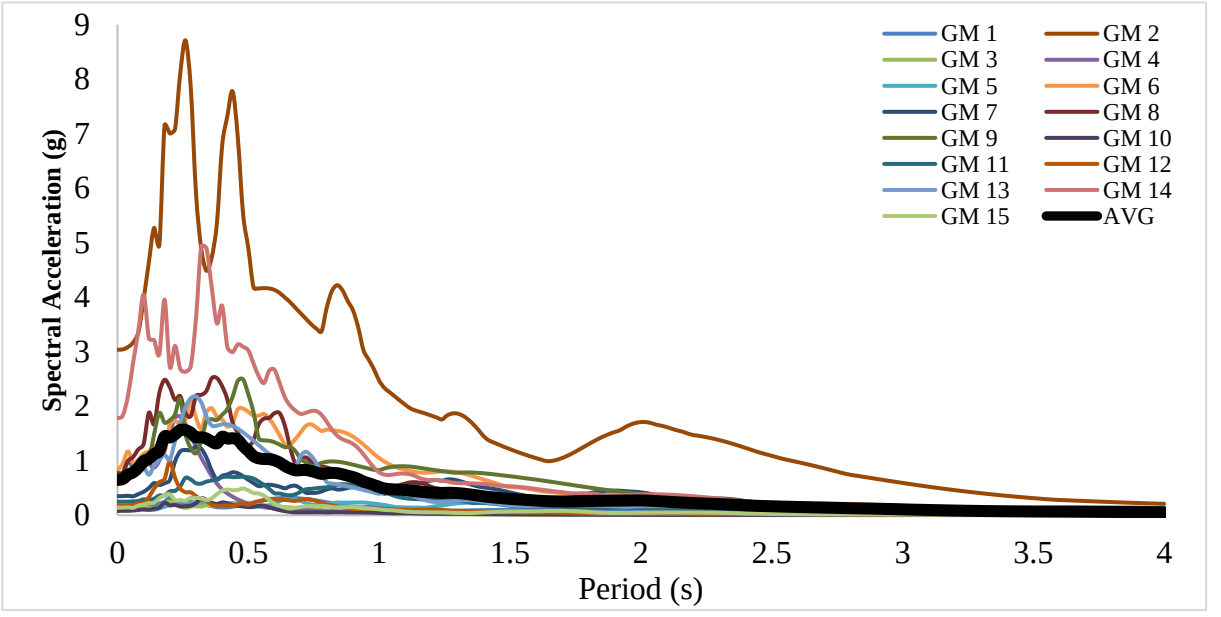

Fig. 8 Spectra of selected ground motions.

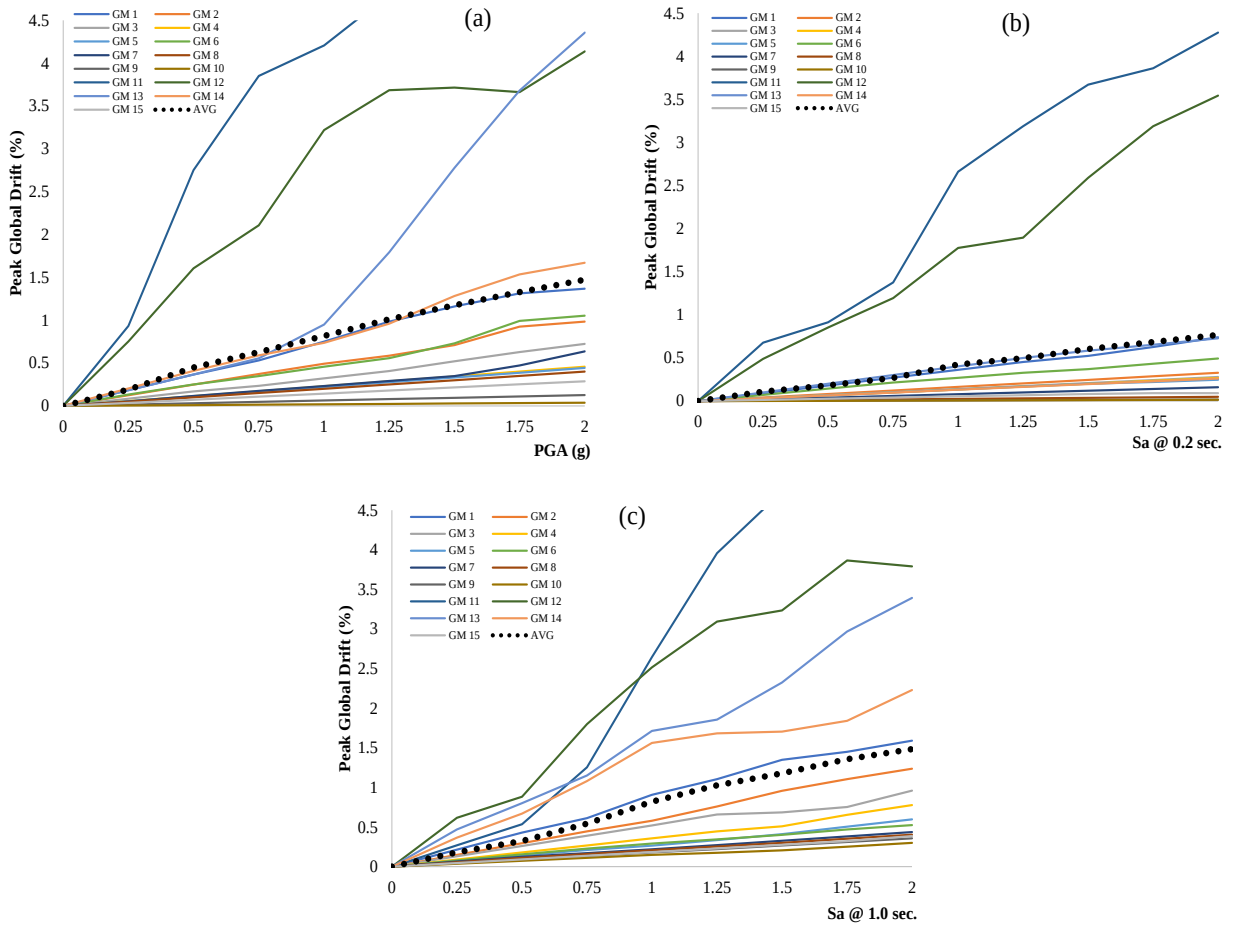

Fig. 9 Results of IDA against all IMs; a) PGA b) S_a @ 0.2 sec. c) S_a @ 1.0 sec.

that inherent variability of different ground motions results in different structural deformational response against the identical value of an IM, indicating the significance for considering the aleatory uncertainties. The black dotted line in Fig. 9 illustrates the average values. Further discussion about the consideration of the uncertainties in the presented work are discussed in Section 4.

4. Fragility analysis

Seismic fragility relationships provide a lucid insight into the structural condition against specific levels of seismic demands as they graphically represent the probabilistic value of being in a specific structural limit or damage state. After obtaining the results from analytical simulations, they can be post-processed to obtain the fragility curves; however, it is imperative to incorporate the uncertainties involved in the analyses of structures. The uncertainties can be classified into two broader categories *i.e.*, aleatory, and epistemic. The aleatory uncertainties represent the intricate and intrinsic variability involved in the ground motions *i.e.*, every ground motion induces different results against the same level of seismic intensity due to their frequency distribution and other associated features, and thus, it cannot be ignored. On the other hand, epistemic uncertainties characterize the uncertainties associated with the lack of human knowledge *i.e.*, the variability in the strength of materials. Nevertheless, B. R. Ellingwood and Kinali[43] have investigated vigorously the effect of epistemic uncertainties on the fragility curves and eventually concluded that it does not affect substantially the probability values and the inherent nature of the ground motions is the parameter that influences the overall structural vulnerability. Thus, since the presented study is specifically targeted to assess the structural vulnerability against seismic motions, the aleatory uncertainties have been meticulously taken into account by selecting the ground motions that can be distinctively distinguished from each other, so that the influence of distance-from-epicenters, local geological conditions, different source-mechanisms, varying seismic motion frequency contents, and path attenuations could be incorporated while producing the fragility relationships. The incorporation of aleatory uncertainties is crucial to obtain to a realistic and diverse range of possible outcomes during vulnerability assessment, enabling informed decision-making specifically for strengthening and repairs. Considering the

research conducted by Ellingwood and Kinali[43] that stated the consideration of epistemic uncertainties for buildings have only a trivial and essentially negligible influence on the global fragility, the current work primarily focuses upon characterizing the aleatory uncertainties that control the overall structural vulnerability due to the inherent randomness and stochastic independence of seismic motions.

As stated earlier, for fragility analysis, it is essential to have discreet limit states so that they can be correlated with the structural assessment or its damaged condition by means of an EDP. The following section describes the structural limit states and the EDP in the presented study.

4.1 Structural Limit States and EDP

Limit states characterize the structural damage condition against the corresponding EDPs. The limit states can be defined qualitatively and quantitatively. The qualitative definitions of LS establish the theoretical background for prevailing structural damage condition, while the quantitative definitions are based on the correlation of structural damage with the mathematical value of an EDP. The limit states are further utilized to establish fragility curves that graphically present the probability of being in or exceeding a specific limit state against discreet value of seismic intensity. For instance, the HAZUS[44] establishes the qualitative definitions for four structural damage states namely slightly damaged, moderately damaged, extensively damaged, and completely collapsed against global deformational response. Similarly, Sun *et. al*.[45] established the fragility curves using local nonlinearities and inter-story drift as the EDPs for four limit states, negligible, light, moderate, and severe damage. Vasileiadis *et. al*.[46] assessed the seismic fragility of reinforced concrete (RC) Frames while considering the effect of masonry infills using four damage state *i.e.*, moderate, extensive, and collapse with inter-story drift ratio as the EDP. Analogously, Khan *et. al*.[47] employed three damage states; Immediate Occupancy (IO or LS1), Life Safety (LS or LS2), and Collapse Prevention (CP or LS3) as the limit states against global drift as EDP. For the presented study, the global deformation based response has been taken as the EDP against three limit states *i.e.* LS1, LS2, and LS3. The initialization of yielding of longitudinal steel anywhere in the structure is taken as the threshold for being in the first damage states *i.e.* LS1, while the third damage states (LS3) is taken as the 75% of the ultimate deformation as suggested by Erberik.[48] The second limit state *i.e.* LS2 has been considered as 75% of the third state (LS3) mathematically. Thus, the LS1 is characterized by the force arising in the structure, and LS3 is characterized by the deformation in the structure, and LS1 is the combination of force and displacement based response. The qualitative definitions for all these limit states have been kept consistent for all the considered modes, while the quantitative definitions are varied in accordance with the discreet modal response as per their monotonic pushover curves, presented in Fig. 4. The quantitative or mathematical definitions of presented limit states are given in Table 4 for the considered modes.

Table 4. Quantitative definition of presented limit states against EDP.

Mode No.	Limit State (%) - Global Drift (EDP)		
	Immediate Occupancy (LS1)	Life Safety (LS2)	Collapse Prevention (LS3)
1	0.68	2.80	3.70
2	0.11	0.28	0.38
3	0.045	0.135	0.18

4.2 Fragility curves development

After obtaining the results from IDA, the results have been processed to attain probabilities for seismic fragility curves. Once the computed peak drifts reach the mathematical threshold of EDP in any of the modes against the specified LS, an event is statistically counted for the calculation of probability against whole sample, consisting of all ground motions. Thus, direct sampling probabilities were attained over the selected GMs against each IM. A lognormal distribution was assumed for regressing the fragility curves in accordance with the following equation:

$$P(LS|IM) = \Phi\left(\frac{lnIM - \lambda_c}{\beta_c}\right) \quad (2)$$

In the above equation, the probability of being in a LS is represented by $P(LS|IM)$, *whereas* Φ is the cumulative distribution function (CDF) to represent graphical curve, and λ_c and β_c represent the median and standard deviation of the CDF, which were optimized using Maximum Likelihood Method (MLM)[49] to develop the best possible fit for developed fragility relationships. Fig. 10 presents the established fragility curves for considered building and for eventual comparison with the results obtained by implementing ML algorithms.

The subsequent section describes the development and implementation of different ML algorithms for producing the fragility relationships of tubular structures using the simulation results of IDA by considering both structural and seismic parameters, as the inputs.

5. ML based seismic fragility assessment of high-rise structures

In the presented study, ML based algorithms have been

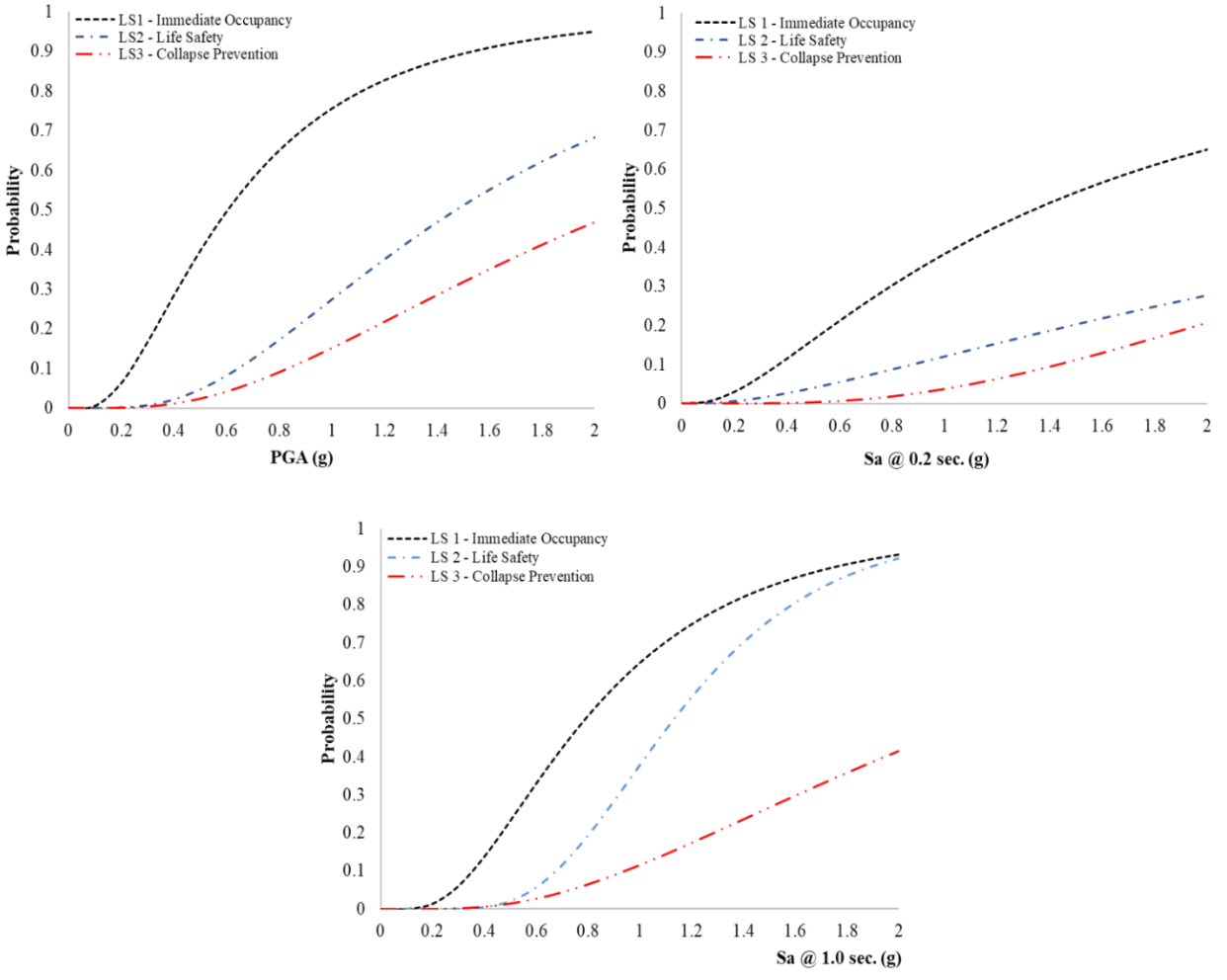

Fig. 10 Seismic fragility curves developed using IDA.

developed to predict the seismic vulnerability of tubular high-rise structures. The results obtained from IDA have been used to train four different ML models including Artificial Neural Network (ANN), Decision Tree (DT), Random Forest (RF), and K-nearest neighbor (KNN). Conventionally, only seismic inputs are considered to develop ML models, however, in the presented study, the input parameters also include the structural characteristics so that generically applicable algorithms could be developed, and their practical efficiency and applicability could be evaluated. Analogous LS has been used for this part of the paper, and a total of 10 parameters have been used as the input with peak drift values as the final outputs from all considered ML algorithms. For the training of the algorithms, 80% of the whole data has been used, while rest of the 20% data has been utilized for testing and performance evaluation purpose. The input parameters for structural characteristics and seismic actions are discussed in detail in the proceeding subsection.

5.1 Input parameters

The input parameters consist of the structural parameters, as well as the seismic parameters. For using the structural parameters as an input, the total height of the building, number of stories; number of podium floors, number of tower's building floors, podium plan area, podium floor heights, typical floor area, typical floor height, and typical areas of core walls in podium and upper floors are considered. The seismic input parameters have been kept consistent with the ones used during the vulnerability assessment process in the preceding sections of this paper so that a comparison can be drawn between the fragility curves obtained in the preceding section and the ones developed using ML algorithms.

The parameters have been selected on their discreet pertinence to overall structural fragility. The areas of shear walls control the structural response against seismic motions, thus, controlling the overall base shear, while the flooring characteristics including the story heights characterize the deformational features of the buildings. On the other hand, the seismic parameters designate the seismic forces, a structure may experience. The selected input parameters substantially influence the ML models' capability to identify the nexus between building features, seismic forces, and building's

overall susceptibility to dynamic seismic loading, thus resulting in adequate structural vulnerability predictions. As the target output variable, the drift has been considered. Drifts directly reflect the structural responsivity to seismic forces, correlates well with the observed structural damage, and can be considered to identify the global failure or collapse, which cannot be predicted by member level forces. The input parameters are summarized in Table 5.

Table 5. Input parameters for ML algorithms.

Input Parameters for ML Algorithms	
Structural Parameters	Total height of the building Number of stories Number of podium floors Number of tower building floors Podium plan area Podium floor heights Typical floor area Typical floor height Typical areas of shear walls in podium Typical areas of shear walls in upper floors
Seismic Input Parameters	Peak Ground Acceleration (PGA) Spectral Acceleration at 0.2 Sec. (Sa @ 0.2 sec.) Spectral Acceleration at 1.0 Sec. (Sa @ 1 sec.)

5.2 ML algorithms

The ML algorithms of RF, SVM, DT, KNN, and ANN are developed in this study for establishing fragility curves of tubular structures with Scikit-Learn library.

Scikit-Learn library allows pristine resources for data preprocessing, normalization, data cleaning, algorithm selections, and fine-tune the chosen algorithms for modelling, training, and evaluation of the data. Furthermore, it also provides tremendous tools for assessing the models' accuracy through performance metrics. In the current work, performance of developed algorithms has been evaluated by means of model metrics *i.e.*, recall, precision, accuracy and F1 score, which have been calculated using the parameters as exhibited in Table 6. These metrics characterize the capability of trained algorithms to distinguish the data of interest (positive) from the residual (negative). Recall characterizes the models' ability to correctly predict the instances' belonging to a specific class of data and typically varies between 0 and 1, with 1 being the most successful identification of all positive instances. On the other hand, precision evaluates the actual number of positive instances out of the predicted positive instances. The precision range of values also lies between 0 and 1, with 0 indicating the bitter performance of models, while the value of 1 indicating the best performance of the algorithm in question. F1-Score, on the other hand, incorporates the combination of recall and precision in a single value by producing a harmonic means as illustrated in Table 6.

The accuracy of established algorithms has been evaluated in accordance with the following equation:

$$Accuracy = \frac{TP+TN}{TP+FP+FN+TN} \quad (3)$$

where TP, TN, FP, and FN are described in Table 6.

5.2.1 Accuracy of ML Models for Predicting Global Drifts

The performance of developed algorithms has been evaluated using the model metrics. The limit states, classified correctly by the algorithms, are represented by the diagonals, while the incorrected limit states are characterized by off-diagonal elements. The graph between predicted and actual

Table 6. Confusion metrics parameters for evaluating the performance of algorithms.

Predicted Class*		Model Metrics	
Yes	No	Recall (R)	$\frac{True\ Positive\ (TP)}{True\ Positive\ (TP) + False\ Negative(FN)}$
True Positive (TP)	False Negative (FN)	Precision (P)	$\frac{True\ Positive\ (TP)}{True\ Positive(TP) + False\ Positive(FP)}$
False Positive (FP)	True Negative (TN)	F1-Score	$\frac{2\ X\ R\ X\ P}{R + P}$

*Description:
TP = Positively labelled data points that are positive
FP = Positively labelled data points that are negative
FN = Negatively labelled data point that are positive
TN = Negatively labeled data points that are negative

drift values is shown in Fig. 11 against PGA. The algorithms were trained with 80% of the dataset, while 20% of the data was used for testing purpose.

Table 7 shows the comparison among employed algorithms for predicting global drifts. It is pertinent to mention that ANN resulted in the most appropriate correlation coefficient with value of 0.9972 while predicting the drifts, whereas SVM resulted in the least accurate correlation with 0.8838.

Before developing the ML models, the datasets were normalized to establish a rational comparison among the developed ML algorithms. From Table 7, it can be inferred that ANN has exhibited lower error metrics and higher correlation coefficients during training and testing phases, however, despite good generalization, a slighter drop could be observed in the ANN model's performance. On the other hand, SVM has yielded higher error metrics and lower correlation coefficients of 0.8838 and 0.4698 in training and testing phases respectively. Thus, the SVM seemed to encounter higher difficulty for generalization, and resultantly overfitting in the results. The DT and KNN have also exhibited good correlation coefficients with a moderate level of error, depicting a reasonable generalization to the testing dataset. From all the ML models, RF has demonstrated the highest correlation coefficients in both datasets *i.e.*, training and testing datasets, depicting its highly capable generalization capabilities. These variations in the performance of considered ML models can be attributed to several factors including ML algorithms capability and capacity of identifying the hidden data patterns. For instance, ANN and RF models are highly flexible to identify and model the convoluted data patterns, whereas SVM is a relatively simple ML algorithm that may struggle with complicated datasets and data interconnections. Similarly, RF is considered to be more robust towards the data's irrelevant characteristics, while it has been observed through the lower correlation coefficients that SVM could have been sensitive to statistically outlying structural drifts under extreme seismic events. Furthermore, the higher error metrics of SVM in comparison with other ML models in presented study would also have been resulted from its lower suitability to specific features of structural response data as SVM may not perform well in the nonlinear data models, whereas the RF and ANN models have handled the data with adequate accuracy. By implementing the established algorithms, the fragility assessment was made, and its details are mentioned in the subsequent section.

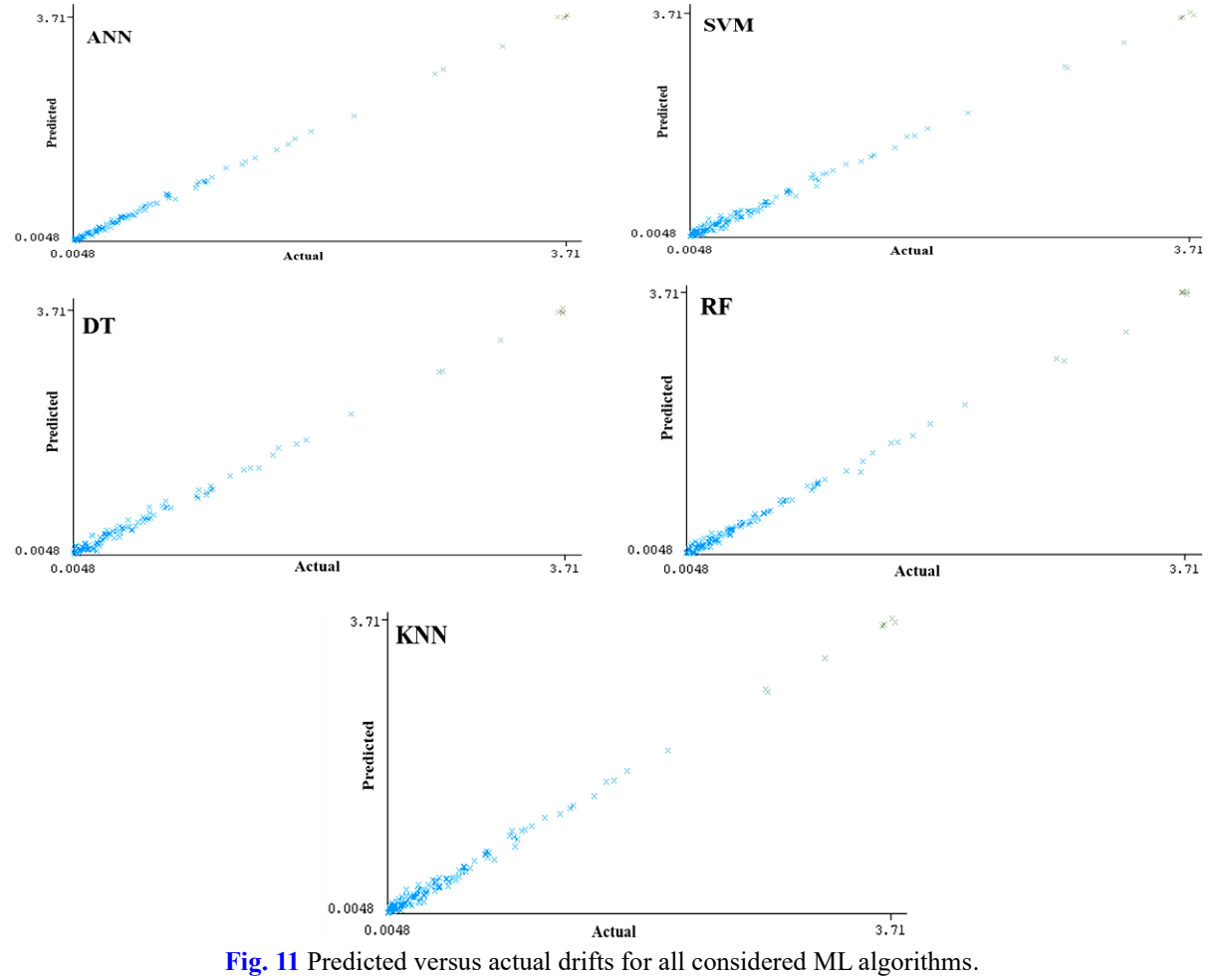

Fig. 11 Predicted versus actual drifts for all considered ML algorithms.

Table 7. Correlation comparison among employed algorithms.

Algorithm	Training Set			Testing Set		
	Correlation Coefficient	Mean Absolute Error	Root Mean Squared Error	Correlation Coefficient	Mean Absolute Error	Root Mean Squared Error
ANN	0.9972	0.1093	0.1391	0.9804	0.1303	0.2106
SVM	0.8838	0.3328	0.7199	0.4698	0.5536	1.1903
DT	0.895	0.3273	0.6829	0.7277	0.4792	1.061
RF	0.9975	0.0578	0.1126	0.908	0.1816	0.4691
KNN	0.9687	0.1358	0.1581	0.9103	0.2189	0.4632

5.2.1 Accuracy of ML Models for fragility assessment

The ML models have been tested for predicting the overall structural fragility against PGA as an IMs because it is more conventionally and commonly understandable. The confusion matrices for all limit states against PGA as an IM are presented in Fig. 12. The schematics for TP, FN, FP, and TN are also mentioned in the same figure for better understandability of readers. It has been observed that ANN can correctly predict 20 instances for LS1, 21 instances for LS2, and 19 instances for LS3 on the testing dataset, resulting in an overall accuracy of 86.95%, 91.30%, and 82.61% for predicting LS1, LS2, and LS3, respectively.

The overall accuracy of 86.95% is obtained for predicting correct instances by using ANN for all limit states. Similarly, the accuracy for SVM, DT, RF, and KNN are 88.40%, 69.56%, 93.05%, and 88.80%, respectively. The performance metrics of employed ML algorithms are illustrated in Table 8, which including recall, precision, and F1-scores. Obtained results amply stipulates the capability of employed algorithms in predicting the overall seismic vulnerability. The performance metrics substantiate that these algorithms can be used to predict the seismic fragility of structures with adequate accuracy. The prediction results of LS1 shows similar, and coinciding values in performance metrics as most of the obtained structural drifts pass the threshold EDP limit for LS1. Overall, RF results in the highest accuracy and F1-scores while predicting the seismic fragility, substantiating its employability for predicting structural vulnerability of high-rise buildings using ML algorithms.

Table 8. Performance metrics of employed ML algorithms.

Limit State	Algorithm					
		ANN	SVM	DT	RF	KNN
LS 1	Precision	0.750	1.00	1.00	1.00	0.857
	Recall	0.857	0.571	0.571	0.867	0.857
	F1-Score	0.800	0.727	0.727	0.867	0.857
LS 2	Precision	0.889	0.97	0.77	0.99	0.90
	Recall	0.800	0.80	0.62	0.90	0.929
	F1-Score	0.842	0.889	0.69	0.947	0.929
LS 3	Precision	0.833	0.773	0.708	0.944	0.895
	Recall	0.882	0.88	0.889	1.0	1.0
	F1-Score	0.857	0.872	0.829	0.971	0.944

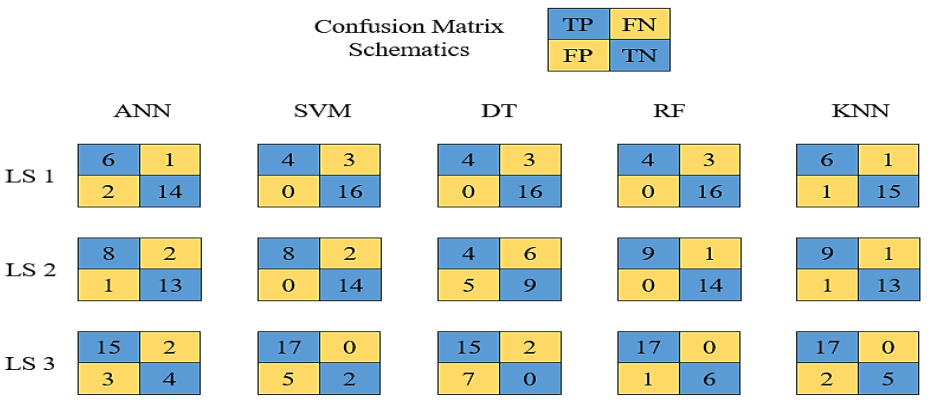

Fig. 12 Confusion Matrix for employed ML algorithms.

The results obtained from implementing the ML algorithms are processed to establish fragility functions as displayed in Fig. 13. Fragility curves exhibit the graphical presentation of exceeding a probability value against discreet levels of seismic demands. Fig. 13 shows the comparison of obtained fragility relationships on limit state-basis through IDA and employed ML algorithms against PGA as the IM. The median and standard deviations of fitted fragility functions are established using MLM as illustrated in Baker[49] and are presented in Table 9. The first column in Table 9 represents the median (λ), and standard deviation (β) of the fitting parameters. The efficacy of ML algorithms is quite evident from established fragility relationships. Since the curves are closely matched and sometimes overlapping with the structural response from engineering analyses, it is advisable to see the online version of the manuscript to distinguish the fragility curves obtained from different ML models. It is pertinent to mention that algorithms achieved higher accuracy for training datasets, while a lesser accuracy was observed while executing the testing datasets. In all algorithms, DT has shown the lowest recall value of 57% for LS1, while for other limit states, it exhibited little higher values; however, resulting in the lower overall accuracy, which can be attributed to the various and consistent small changes in the training data of deformational structural response, leading to lesser accuracy in predictions due to different tree structures. For LS1, RF achieved the highest recall value with the highest overall accuracy. For predicting the collapse level limit state, both KNN and RF resulted in the similar and highest recall values, however, RF attained a higher value of F1-score, depicting its overall better performance in predicting the collapse limit state. For collapse limit state, LS3, ANN attained an overall recall of 88%. The ML algorithms performed substantially well in predicting the structural vulnerability for the tubular structure.

6. Comparison between ML models and traditional engineering analyses: advantages, limitations, and trade-offs

ML algorithms can identify the convoluted data patterns which can be challenging for traditional engineering analyses methods, thus reducing the computational time for subsequent vulnerability assessments with similar types of seismic demands and structural characteristics. Furthermore, the ML models can reliably handle the nonlinear structural responses which are common during seismic events, while traditional engineering methods require extensive computational resources to capture this behavior. Moreover, employing ML models can be trained to automate the process for establishing seismic fragility curves to substantially reduce the conventional manual efforts.

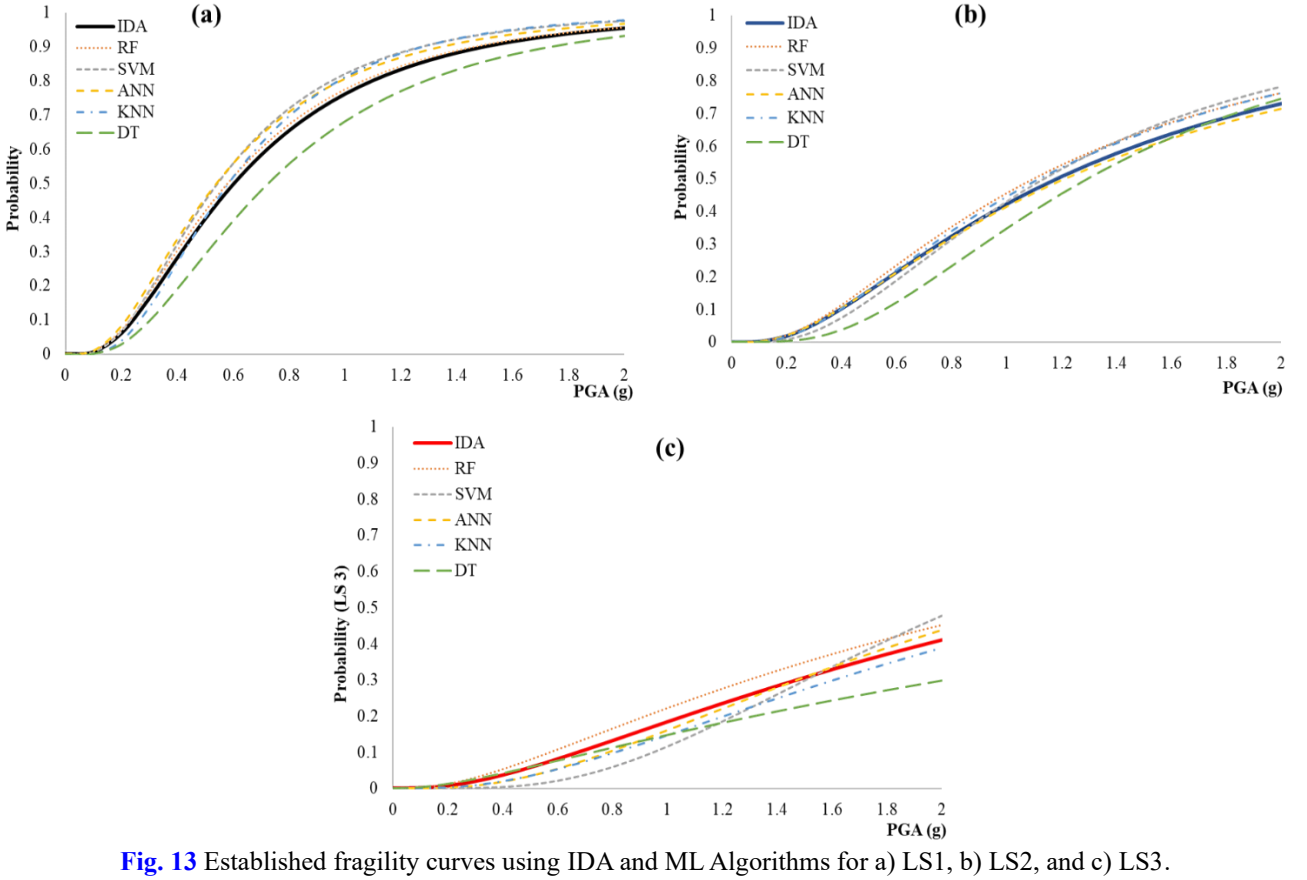

Fig. 13 Established fragility curves using IDA and ML Algorithms for a) LS1, b) LS2, and c) LS3.

Table 9. Fragility curves parameters.

Fitting Parameter	IDA		ANN		SVM		DT		RF		KNN	
	λ	β	λ	β	λ	β	λ	β	λ	β	λ	β
LS 1	0.60	0.71	0.54	0.71	0.54	0.66	0.72	0.68	0.58	0.71	0.58	0.61
LS 2	1.18	0.85	1.20	0.88	1.13	0.72	1.29	0.65	1.09	0.84	1.11	0.81
LS 3	2.52	1.02	2.27	0.82	2.07	0.60	4.07	1.34	2.27	1.07	2.57	0.90

However, despite serving as extensive tools to produce seismic vulnerability information, the ML models heavily rely upon elaborate engineering analysis for training purposes. Thus, during unforeseen statistically outlying seismic events, which may trigger unprecedented structural responses, the ML models may limit the models' application for predicting the structural vulnerability. Furthermore, as the ML algorithms are trained on existing datasets that may exhibit a specific data pattern, the ML models may not respond well to different seismic loading conditions and correspondingly disparate structural responses, resulting in limited generalized applicability. Moreover, traditional engineering analyses methods have established validation methodologies, while the results from ML models are difficult to validate.

Not only the tall building is concerned, our today's buildings, several construction types such as prefabrication, additive manufacturing, lightweight concrete construction, digital fabrication,[50-52] but the variability of the obtained dataset can also be extreme. The structural vulnerability against seismic loading in the traditional engineering analyses methods is inefficient and somewhat impossible. The applicability of ML models to predict the structural vulnerability against seismic loading is beneficial for the wide range of special buildings as they provide data-driven insights with incorporation of multi-faceted data and can be trained discreetly to assess the structural seismic vulnerability of various types of structures including complex wall-frame interaction.

7. Conclusion

In the present work, the efficacy of ML algorithms including ANN, SVM, DT, RF, and KNN has been evaluated to establish fragility curves for super tall buildings. The conclusions were drawn below:

- The RF and ANN algorithms have offered substantial potential for higher reliability.
- Elaborated predictive capability was shown by RF and ANN, surpassing other ML algorithms. For the problem at hand, the highest overall accuracy of 93.05% was achieved for RF due to its capability for ensemble learning, and robustness to variability.
- Reasonable higher correlation coefficients of DT and KNN, exhibiting good generalization, however, SVM resulted in lower correlation coefficients due to its limited capability of handling nonlinear data and pertinent noisy characteristics.
- The predicted values were compared with the actual values, and results were promising for structural vulnerability prediction.

In structural engineering, accuracy in structural vulnerability assessment is vital to establish risk mitigation mechanisms. As potentially identified through this work, the higher performing ML models, such as RF and ANN, can be utilized to automate the structural vulnerability assessment process in real-time scenarios to identify the needs for structural optimization and retrofitting measures. The derived insights from the presented work can be utilized to extend the application of tested ML models to other categories of complex building structures. Despite the variation in design parameters and particular structural configurations, the rudimentary basis established in this study for vulnerability assessment would remain pertinent. The potentially identified ML models of RF and ANN can be utilized to extend the implementation on other diverse typologies of building structures. This vulnerability assessment scheme can be adapted and extended to use in other seismically activated regions. Versatile geological and ground motion characteristics can be considered to utilize the presented ML models with consistent foundational approach, and retraining or recalibration can be executed for adequately accurate results. Thus, the consistent and continuous research in the implementation of ML models to structural engineering can directly impact real-world scenarios by ensuring safer and resilient infrastructure. Without doubt, the integration of real-time monitoring of buildings during earthquake events, better and well-informed decision making will be possible to safeguard the lives. However, establishing more elaborate training datasets *i.e.*, consideration of versatile types of plans, soil structure interaction, and seismic pounding, shall be needed to produce better accuracy and reliability of results.

For future research, integrated hybrid analyses methodologies can be developed that may leverage from the combination of ML models with conventional engineering analyses for structural health monitoring and vulnerability

assessments. The amalgamation of versatile ML models and traditional engineering methods would not only reduce the overall complexity and computational burden of vulnerability assessment process, but it will also result in developing better early warning systems and resilient communities.

Acknowledgement

The authors would like to thank the "Chulalongkorn Academic Advancement into its Second Century Fund (C2F) for Postdoctoral Fellowship (Z. Muhammad). This project is also funded by National Research Council of Thailand (NRCT) and Chulalongkorn University (Grant No. N42A660629). This research is also funded by Thailand Science Research and Innovation Fund Chulalongkorn University (SOCF67250015).

Conflict of Interest

There is no conflict of interest.

Supporting Information

Not applicable.

References

[1] S. Ali Memon, M. Zain, D. Zhang, S. K. U. Rehman, M. Usman, D. Lee, Emerging trends in the growth of structural systems for tall buildings, *Journal of Structural Integrity and Maintenance*, 2020, **5**, 155-170, doi: 10.1080/24705314.2020.1765270.

[2] M. Zain, M. Usman, S. H. Farooq, A. Hanif, Progressive structural capacity loss assessment—a framework for modern reinforced concrete buildings, *PLoS One*, 2018, **13**, e0208149, doi: 10.1371/journal.pone.0208149.

[3] W. Tuvayanond, L. Prasittisopin, Design for manufacture and assembly of digital fabrication and additive manufacturing in construction: a review, *Buildings*, 2023, **13**, 429, doi: 10.3390/buildings13020429.

[4] T. Thwe Win, P. Jongvivatsakul, T. Jirawattanasomkul, L. Prasittisopin, S. Likitlersuang, Use of polypropylene fibers extracted from recycled surgical face masks in cement mortar, *Construction and Building Materials*, 2023, **391**, 131845, doi: 10.1016/j.conbuildmat.2023.131845.

[5] L. Prasittisopin, T. Sakdanaraseth, V. Horayangkura, Design and construction method of a 3D concrete printing self-supporting curvilinear pavilion, *Journal of Architectural Engineering*, 2021, **27**, doi: 10.1061/(asce)ae.1943-5568.0000485.

[6] M. Zain, M. Usman, S. H. Farooq, T. Mehmood, Seismic vulnerability assessment of school buildings in seismic zone 4 of Pakistan, *Advances in Civil Engineering*, 2019, **2019**, 1-14, doi: 10.1155/2019/5808256.

[7] J. Ji, A. S. Elnashai, D. A. Kuchma, An analytical framework for seismic fragility analysis of RC high-rise buildings, *Engineering Structures*, 2007, **29**, 3197-3209, doi: 10.1016/j.engstruct.2007.08.026.

[8] J. Park, P. Towashiraporn, J. I. Craig, B. J. Goodno, Seismic fragility analysis of low-rise unreinforced masonry structures, *Engineering Structures*, 2009, **31**, 125-137, doi: 10.1016/j.engstruct.2008.07.021.

[9] I. Ioannou, R. E. Chandler, T. Rossetto, Empirical fragility curves: the effect of uncertainty in ground motion intensity, *Soil Dynamics and Earthquake Engineering*, 2020, **129**, 105908, doi: 10.1016/j.soildyn.2019.105908.

[10] M. Biglari, A. Formisano, Damage probability matrices and empirical fragility curves from damage data on masonry buildings after sarpol-e-zahab and bam earthquakes of Iran, *Frontiers in Built Environment*, 2020, **6**, 2, doi: 10.3389/fbuil.2020.00002.

[11] A. Rosti, C. Del Gaudio, M. Rota, P. Ricci, M. Di Ludovico, A. Penna, G. M. Verderame, Empirical fragility curves for Italian residential RC buildings, *Bulletin of Earthquake Engineering*, 2021, **19**, 3165-3183, doi: 10.1007/s10518-020-00971-4.

[12] S. Argyroudis, A. M. Kaynia, K. Pitilakis, Development of fragility functions for geotechnical constructions: application to cantilever retaining walls, *Soil Dynamics and Earthquake Engineering*, 2013, **50**, 106-116, doi: 10.1016/j.soildyn.2013.02.014.

[13] M. Altug Erberik, Seismic fragility analysis. Encyclopedia of Earthquake Engineering. Berlin, Heidelberg: Springer Berlin Heidelberg, 2015: 1-10, doi: 10.1007/978-3-642-36197-5_387-1.

[14] K. Pitilakis, S. Argyroudis, Seismic vulnerability assessment: lifelines. Encyclopedia of Earthquake Engineering. Berlin, Heidelberg: Springer Berlin Heidelberg, 2014: 1-33, doi: 10.1007/978-3-642-36197-5_255-1.

[15] M. T. Schultz, B. P. Gouldby, J. D. Simm, Beyond the Factor of Safety: Developing Fragility Curves to Characterize System Reliability, *Engineer Research and Development Center*, 2010.

[16] A. Stocchi, C. Giry, S. Capdevielle, I. Zentner, E. Nayman, F. Ragueneau, A simplified non-linear modelling strategy to generate fragility curves for old masonry buildings, *Computers & Structures*, 2021, **254**, 106579, doi: 10.1016/j.compstruc.2021.106579.

[17] P. Zhai, P. Zhao, Y. Lu, C. Ye, F. Xiong, Seismic fragility analysis of buildings based on double-parameter damage models considering soil-structure interaction, *Advances in Materials Science and Engineering*, 2019, **2019**, 1-13, doi: 10.1155/2019/4592847.

[18] S. Jin, Z. Li, Z. Dong, T. Lan, J. Gong, A simplified fragility analysis methodology for containment structure subjected to overpressure condition, *International Journal of Pressure Vessels and Piping*, 2020, **184**, 104104, doi: 10.1016/j.ijpvp.2020.104104.

[19] M. Zain, M. Usman, S. Hassan Farooq, A Framework with reduced computational burden for Seismic Fragility Assessment of Reinforced Concrete Buildings in High-Intensity Seismic Zones, *Structures*, 2021, **33**, 3055-3065, doi: 10.1016/j.istruc.2021.06.050.

[20] A. Raj, C. Ngamkhanong, L. Prasittisopin, S. Kaewunruen, Nonlinear dynamic responses of ballasted railway tracks using

concrete sleepers incorporated with reinforced fibres and pre-treated crumb rubber, *Nonlinear Engineering*, 2023, **12**, doi: 10.1515/nleng-2022-0320.
[21] J. Kiani, C. Camp, S. Pezeshk, On the application of machine learning techniques to derive seismic fragility curves, *Computers & Structures*, 2019, **218**, 108-122, doi: 10.1016/j.compstruc.2019.03.004.
[22] A. Rasheed, M. Usman, M. Zain, N. Iqbal, Machine learning-based fragility assessment of reinforced concrete buildings, *Computational Intelligence and Neuroscience*, 2022, **2022**, 1-12, doi: 10.1155/2022/5504283.
[23] Peng, Huang, Machine learning approach for investigating compressive strength of self-compacting concrete containing supplementary cementitious materials and recycled aggregate, *Journal of Building Engineering*, 2023, **79**, 107904, doi: 10.1016/j.jobe.2023.107904.
[24] M. M. Hameed, M. K. AlOmar, W. J. Baniya, M. A. AlSaadi, Incorporation of artificial neural network with principal component analysis and cross-validation technique to predict high-performance concrete compressive strength, *Asian Journal of Civil Engineering*, 2021, **22**, 1019-1031, doi: 10.1007/s42107-021-00362-3.
[25] W. Kittinaraporn, S. Tuprakay, L. Prasittisopin, Effective modeling for construction activities of recycled aggregate concrete using artificial neural network, *Journal of Construction Engineering and Management*, 2022, **148**, doi: 10.1061/(asce)co.1943-7862.0002246.
[26] Sujith, Mangalathu, Classification of failure mode and prediction of shear strength for reinforced concrete beam-column joints using machine learning techniques, *Engineering Structures*, 2018, **160**, 85-94, doi: 10.1016/j.engstruct.2018.01.008.
[27] D.-W. Jia, Z.-Y. Wu, Structural probabilistic seismic risk analysis and damage prediction based on artificial neural network, *Structures*, 2022, **41**, 982-996, doi: 10.1016/j.istruc.2022.05.056.
[28] B. Todorov, A. H. M. Muntasir Billah, Post-earthquake seismic capacity estimation of reinforced concrete bridge piers using Machine learning techniques, *Structures*, 2022, **41**, 1190-1206, doi: 10.1016/j.istruc.2022.05.067.
[29] Z. Wang, Y.-J. Cha, Unsupervised machine and deep learning methods for structural damage detection: a comparative study, *Engineering Reports*, 2022, e12551, doi: 10.1002/eng2.12551.
[30] C. M. Wen, S. L. Hung, C. S. Huang, J. C. Jan, Unsupervised fuzzy neural networks for damage detection of structures, *Structural Control and Health Monitoring*, 2007, **14**, 144-161, doi: 10.1002/stc.116.
[31] K. A. Eltouny, X. Liang, Bayesian-optimized unsupervised learning approach for structural damage detection, *Computer-Aided Civil and Infrastructure Engineering*, 2021, **36**, 1249-1269, doi: 10.1111/mice.12680.
[32] S. Shi, D. Du, O. Mercan, E. Kalkan, S. Wang, A novel unsupervised real-time damage detection method for structural health monitoring using machine learning, *Structural Control and Health Monitoring*, 2022, **29**, e3042, doi: 10.1002/stc.3042.
[33] K. Eltouny, M. Gomaa, X. Liang, Unsupervised learning methods for data-driven vibration-based structural health monitoring: a review, *Sensors*, 2023, **23**, 3290, doi: 10.3390/s23063290.
[34] H. T. Mai, Q. X. Lieu, J. Kang, J. Lee, A novel deep unsupervised learning-based framework for optimization of truss structures, *Engineering with Computers*, 2023, **39**, 2585-2608, doi: 10.1007/s00366-022-01636-3.
[35] S. Shin, D. Shin, N. Kang, Topology optimization via machine learning and deep learning: a review, *Journal of Computational Design and Engineering*, 2023, **10**, 1736-1766, doi: 10.1093/jcde/qwad072.
[36] R. Zhang, J. Hajjar, H. Sun, Machine learning approach for sequence clustering with applications to ground-motion selection, *Journal of Engineering Mechanics*, 2020, **146**, doi: 10.1061/(asce)em.1943-7889.0001766.
[37] M. Zain, N. Anwar, F. A. Najam, T. Mehmood, Seismic fragility assessment of reinforced concrete high-rise buildings using the uncoupled modal response history analysis (UMRHA). Proceedings of the International Conference on Earthquake Engineering and Structural Dynamics. Cham: Springer International Publishing, 2018: 201-218, doi: 10.1007/978-3-319-78187-7_16.
[38] A. K. Chopra, Dynamics of Structures, *Prentice Hall*, 2004.
[39] D. G. Lignos, Interactive Interface for Incremental Dynamic Analysis: Theory and Example Applications Manual, *McGill University*, 2010.
[40] P. Song, C. Wang, and Q. Sun, Mainshock-aftershock fragility surfaces analysis of reinforced concrete frame structures using a double incremental dynamic analysis approach, *Structures*, 2023, **56**, 104868, doi: 10.1016/j.istruc.2023.07.058.
[41] D.-D. Nguyen, B. Thusa, M. S. Azad, V.-L. Tran, T.-H. Lee, Optimal earthquake intensity measures for probabilistic seismic demand models of ARP1400 reactor containment building, *Nuclear Engineering and Technology*, 2021, **53**, 4179-4188, doi: 10.1016/j.net.2021.06.034.
[42] M. Grigoriu, Do seismic intensity measures (IMs) measure up? *Probabilistic Engineering Mechanics*, 2016, **46**, 80-93, doi: 10.1016/j.probengmech.2016.09.002.
[43] B. R. Ellingwood, K. Kinali, Quantifying and communicating uncertainty in seismic risk assessment, *Structural Safety*, 2009, **31**, 179-187, doi: 10.1016/j.strusafe.2008.06.001.
[44] Hazus Earthquake Model Technical Manual, *Federal Emergency Management Agency (FEMA)*, 2022.
[45] B. Sun, Y. Zhang, D. Dai, L. Wang, J. Ou, Seismic fragility analysis of a large-scale frame structure with local nonlinearities using an efficient reduced-order Newton-Raphson method, *Soil Dynamics and Earthquake Engineering*, 2023, **164**, 107559, doi: 10.1016/j.soildyn.2022.107559.
[46] V. Vasileiadis, K. Kostinakis, A. Athanatopoulou, Story-wise assessment of seismic behavior and fragility analysis of R/C frames considering the effect of masonry infills, *Soil Dynamics and Earthquake Engineering*, 2023, **165**, 107714, doi: 10.1016/j.soildyn.2022.107714.
[47] M. W. Khan, M. Usman, S. H. Farooq, M. Zain, S. Saleem, Effect of masonry infill on analytical fragility response of RC frame school buildings in high seismic zone, *Journal of*

Structural Integrity and Maintenance, 2021, **6**, 110-122, doi: 10.1080/24705314.2020.1865624.
[48] M. Altuğ Erberik, Fragility-based assessment of typical mid-rise and low-rise RC buildings in Turkey, *Engineering Structures*, 2008, **30**, 1360-1374, doi: 10.1016/j.engstruct.2007.07.016.
[49] J. W. Baker, Efficient analytical fragility function fitting using dynamic structural analysis, *Earthquake Spectra*, 2015, **31**, 579-599, doi: 10.1193/021113eqs025m.
[50] L. Prasittisopin, C. Khosakitchalert, P. Vas-Umnuay, W. Pansuk, Lightweight concrete for modular floor structure: survey, experiment, In-field study, *Advances in Civil Engineering Materials*, 2022, **11**, 20220020, doi: 10.1520/acem20220020.
[51] P. Jiramarootapong, L. Prasittisopin, C. Snguanyat, G. Tanapornraweekit, S. Tangtermsirikul, Load carrying capacity and failure mode of 3D printing mortar wall panel under axial compression loading. RILEM Bookseries. Cham: Springer International Publishing, 2020: 646-657, doi: 10.1007/978-3-030-49916-7_65.
[52] L. Prasittisopin, D. Trejo, Performance characteristics of blended cementitious systems incorporating chemically transformed rice husk ash, *Advances in Civil Engineering Materials*, 2017, **6**, 20160001, doi: 10.1520/acem20160001.